Tactile texture rendering for electrostatic friction displays: Incorporation of low-frequency friction model and high-frequency textural model

Kazuya Otake[1], Shogo Okamoto[1,2], Yasuhiro Akiyama[1] and Yoji Yamada[1]

***Abstract*— Tactile texture presentation on touch panels enhances their usability and realizes immersive user interfaces. This study develops a tactile texture rendering method for electrostatic friction displays. The method combines two rendering models for material textures compared with previous studies which focused on either of these two models. One of these models is a physical model that simulates low-frequency frictional signals depending on the exploratory finger velocities and contact loads. The other is an autoregression-based data-driven model for high-frequency textural friction. For user studies, we compared combining the two models with using only the physical model for the four types of materials. Although the effectiveness varied across the materials, the subjectively judged realism and identification of the materials were improved for the combined condition. The new method combining high-frequency textural information and low-frequency physical model-based friction is expected to provide realistic tactile textures for electrostatic surface tactile displays.**

I. Introduction

Touch panels have been a major human–computer interface, and tactile feedback techniques for them, i.e., surface tactile displays, have been studied intensively by many researchers [1]. Methods needed to render tactile textures are among the core techniques. Along with vibrotactile displays, friction-variable tactile displays are suitable for providing tactile feedback to fingers on touch panels. Electrostatic friction displays that generate friction variations on the panel are a type of friction-variable display. Ultrasonic displays constitute another type used to reduce surface friction. Data-driven methods are becoming a popular approach to circumvent the establishment of physical models for contact between fingers and fine textures. These methods were also introduced in the cases of electrostatic friction displays. Accelerations [2] and frictional forces [3] caused by sliding fingers or contactors on material surfaces are typically used to build data-driven models. For example, in [3], a touch pen scanned several types of materials, such as cloths, to collect information on contact forces, based on which neural network models were constructed for individual materials to retain the frequency characteristics of friction signals. The models were evaluated by user studies that focused on the subjective similarities between the actual and virtual material textures.

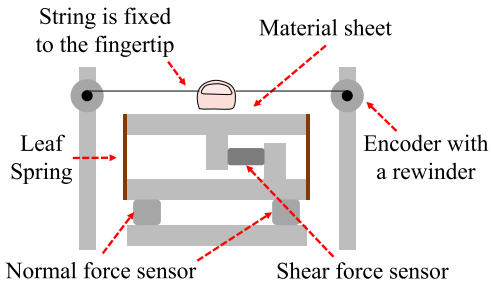

Fig. 1. Schematic of the measurement instrument for the contact force and finger motion. Normal and shear forces were measured by three crystal load cells, and the finger velocity was measured by a pair of encoders.

Earlier studies on data-driven methods [2], [3], [4], [5], [6] focused on surface textures and excluded low-frequency components (e.g., less than 5–10 Hz) for their texture models. This may be partly because some studies used miniature accelerometers that did not properly respond to signals smaller than ∼10 Hz to record vibratory information generated in instances in which a finger slid on textured surfaces. Further, researchers tend to study high-frequency textural stimuli separately from low-frequency stimuli rendered by physical models. For example, in [6], a vibrotactile actuator and force display device were adopted to present high-frequency textural and friction components, respectively.

In this study, we used two types of models concurrently. One is a physical model used to present low-frequency friction forces. The other is a data-driven or frequency-response model that retains the high-frequency frictional properties of textures. No previous study incorporated such two models to cover a wide frequency range for electrostatic surface displays except our earlier work [7]. We adopted previously the simplest Coulomb frictional model to represent low-frequency frictional forces; however, it was ineffective for modeling the finger-material frictions [7]. Furthermore, the high-frequency textural model in [7] did not depend on the finger speed sliding on the touch panel. In the present study, we adopted a physical model for low-frequency signals and an autoregressive model [2], [4], [5] for high-frequency tex-

This study was in part supported by MEXT Kakenhi (20H04263, 21H05819).

[1]Kazuya Otake, Shogo Okamoto, Yasuhiro Akiyama, and Yoji Yamada are with the Department of Mechanical Systems Engineering, Nagoya University, Furocho, Chikusaku, Nagoya 464–8603, Japan

[2]Shogo Okamoto is also with the Department of Computer Sciences, Tokyo Metropolitan University, 6-6, Asahigaoka, Hino, Tokyo, Japan okamotos@tmu.ac.jp

This study was approved by the Institutional Review Board of the School of Engineering, Nagoya University (#20-8).

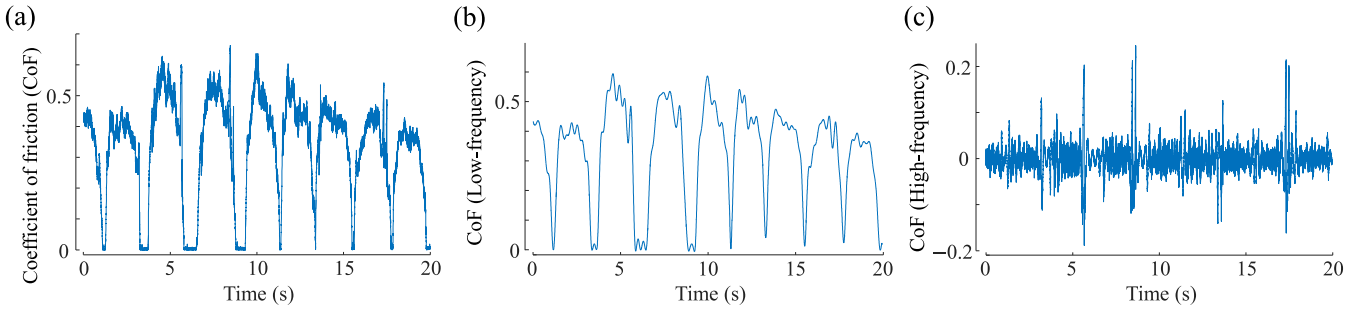

Fig. 2. Coefficient of friction (CoF) when the denim was traced by a finger at a reference velocity of 75 mm/s. (a) CoF recorded when a finger slides over the denim. (b) Low-frequency ($<$ 3.5 Hz) components of CoF. (c) High-frequency ($\geq$ 3.5 Hz) components of CoF. When the CoF is close to zero, the finger does not touch the material.

tural frictions for several finger velocity levels. The method is then evaluated in terms of two viewpoints: subjective realism and texture identification performance based on user tests.

II. Data Collection for Coefficient of Friction

The instrument shown in Fig. 1 was used to measure the two axial forces to derive the coefficient of friction (CoF) and scanning velocity. A similar device was used in our previous study [8]. Two load cells (9313AA2, Kistler, Switzerland, dynamic resolution $=$ 0.01 N) and a high-precision load cell (9217A, Kistler, Switzerland, dynamic resolution $<$ 0.001 N) were used to measure the normal and shear forces, respectively. The interference of the two axial forces was mitigated by the leaf springs fixed to the sides of the instrument. The outputs of the force sensors were amplified by charge amplifiers (5073A and 5015, Kistler, Switzerland for the normal and shear forces, respectively) and transmitted to the computer at 2 kHz. The finger position was measured using a pair of encoders based on a string rewinder mechanism (MTL-12, Microtech Laboratory Inc., Japan). The string attached to the shaft of the encoder was fixed to the first joint of the finger, and the movement of the finger was linked to the rotation of the encoder. Forces to rewind the strings connected to the two encoders were directed opposite to each other and cancelled with each other. Furthermore, the strings were horizontally aligned with the finger, and they did not produce any rewinding forces along the normal direction. These setups hardly interfered with the natural motions and forces of the fingers.

We measured the two-axial forces generated when participants repeatedly traced materials fixed on the upper surface of the measurement apparatus in one direction, that is, left to right in Fig. 1, with the index finger of their dominant hand. Six men in their 20s participated in the measurements after providing written informed consents. The average normal and friction forces of each participant were 0.26–0.96 N and 0.14–0.47 N, respectively. In addition, they adjusted their hand motions to achieve scanning velocities close to 50, 75, 100, 125, and 150 mm/s with feedback displayed on the computer screen. For later data analysis, continuous regions of 100 ms or longer were spliced, wherein the actual velocity was within $\pm$ 20 mm/s for each of these reference velocities. The size of the materials was 100 mm $\times$ 40 mm. For these

Fig. 3. Four types of materials used in the experiments: leather, cork, denim, and wood.

specimens, the forces could be continuously measured for approximately 1 s or less. Hence, the sliding motions were repeated multiple times during a single trial lasting 20 s. For each reference velocity, 10 trials were conducted by individuals. Regarding the normal force, no instructions were given to them. The four types of materials shown in Fig. 3, that is, leather, cork, denim, and wood, were used for data collection. These materials are familiar in our daily lives and exhibit fairly different CoF and surface properties. In our previous study [7], we used a drawing paper; however, it was highly smooth and exhibited minimal textural information. Hence, we replaced the drawing paper with wood in the present study.

The CoF at an instant was calculated as the ratio of the shearing force to the normal force. Only the instants at which the shearing and normal forces were greater than 0.05 N were used. These coefficients of friction were separated into low- and high-frequency components using a Butterworth filter with a cutoff frequency of 3.5 Hz. The cutoff frequency was determined by considering that the natural exploratory hand motion frequencies are only a few Hz [9]. This cutoff frequency was determined such that the coefficient of determination became greatest for the friction model of low-frequency CoF components. As an example, Fig. 2 shows the CoF before and after separation when tracing a denim sheet at a reference velocity of 75 mm/s.

III. Rendering Method

A. Quasistatic friction model

Herein, a quasistatic friction model was introduced to represent the low-frequency ($<$ 3.5 Hz) components of the CoF between the fingers and materials. The CoF between

TABLE I

MEANS AND STANDARD ERRORS OF QUASI-STATIC FRICTION MODEL PARAMETERS.

	a	b	c	d	q
Leather	$.51 \pm .12$	$.36 \pm .13$	$.02 \pm .00$	$.11 \pm .04$	$.89 \pm .05$
Cork	$.35 \pm .04$	$.39 \pm .01$	$.02 \pm .01$	$.18 \pm .08$	$.08 \pm .13$
Denim	$.30 \pm .07$	$.53 \pm .08$	$.03 \pm .01$	$.21 \pm .07$	$.77 \pm .06$
Wood	$.30 \pm .05$	$.32 \pm .08$	$.14 \pm .08$	$.29 \pm .11$	$.87 \pm .07$

the fingers and materials is proportional to the power of the normal force f_n [10], [11], as follows,

$$\mu_p(f_n) = a f_n^b \tag{1}$$

where a and b are constants. Furthermore, the CoF is known as a function of the relative velocity [12],

$$\mu_p(v) = e\frac{1 + dv^q}{1 + cv} \tag{2}$$

where v is the scanning velocity, and c, d, e, and q are constant coefficients. We combined these two models and used

$$\mu_p(f_n, v) = a f_n^b \frac{1 + dv^q}{1 + cv} \tag{3}$$

to approximate the motion-dependent CoF. c and d are zero or positive values, and q ranges from zero to one. As an example, Fig. S1 in Supplemental material presents a comparison of the observed and modeled low-frequency components of CoF.

The model parameters (a–q) were computed using the least-squares method for individual participants and materials. The means and standard errors of the R^2 values for the modeling were 0.38 ± 0.06, 0.52 ± 0.11, 0.47 ± 0.09, and 0.22 ± 0.04 for leather, cork, denim, and wood, respectively. Therefore, in this friction model, 20–50% of the measured CoF could be rendered. Inclusion of dynamic hand motions, such as acceleration in the model, may improve the modeling accuracy. Although this study did not focus on the development of a model of the CoF, it should be updated to a better model in the future.

Table I lists the means and standard errors of the model parameters. In general, the magnitudes of CoF were the highest for the leather, followed by the cork, denim, and wood, whereas the CoF values varied with the hand force and velocity. The mean value of each parameter was used to determine the voltage output of the electrostatic friction display, as described later.

B. Textural friction model above 3.5 Hz

The autoregressive model [4], [5] was used to simulate the frequency response of the textural components above 3.5 Hz in the CoF[1]. As mentioned above, the components (higher than 3.5 Hz) of the CoF collected in Section II were used for this purpose. The model was established for each combination of the five levels of the reference velocity (50, 75, 100, 125, and 150 mm/s) and four types of materials.

To model the average frequency characteristics of the CoF among the six participants, we computed first the fast Fourier transformation of the time series of CoF. The spectra of the six participants were then averaged for each pair of materials and reference velocity. The average spectrum was then inversely converted in the time-series of CoF. These time-series of CoF were used to establish autoregressive models. The autoregressive model was defined by

$$\mu_t(k\Delta t) = \sum_{j=1}^{p} a_j \mu_t((k-j)\Delta t) + w(k\Delta t) \tag{4}$$

where μ_t denotes the high-frequency textural component of the CoF at time $k\Delta t$. Δt is the sampling period: 0.5 ms. The a_j are the coefficients obtained by the Yule–Walker method. w represents the white noise. The textural component $\mu_t(k\Delta t)$ was determined at a certain point in time by a linear combination of past p CoF. p is the order of the model, and was determined based on the Akaike Information Criteria (See the last paragraph of Section V).

We evaluated the similarity between the measured and modeled CoF using a similarity index originally introduced in [5], [13]. According to this index, the mean CoF was well represented although there existed substantial individual differences. The details are summarized in Supplemental material 2.

The frequency responses obtained by the autoregressive model for the four types of materials are shown in Fig. 4. For all materials, the amplitudes at 100, 125, and 150 mm/s were relatively larger than those at 50 and 75 mm/s, and the amplitudes increased as a function of velocity. Findings are comparable to those reported by [14].

IV. EXPERIMENT

A. Apparatus: Electrostatic friction surface display

The electrostatic friction display changes the frictional force by controlling the electrostatic attraction by applying a voltage between the finger pad and panel, as shown in Fig. 5. An insulator exists between the finger pad and panel, and no current flows through the skin. The frictional force varies with the magnitude of the applied voltage and promotes deformation of the finger pad in the shear direction when the finger slides on the panel. Therefore, electrostatic friction stimuli are effective for presenting surfaces in which the frictional force is dominant.

In the experiment, the electrostatic friction display shown in Fig. 6 was used. The electrostatic friction stimuli were presented by applying a voltage between the indium tin oxide (ITO) panel to which an insulating film of 8 μm (kimotect PA8X, Kimoto Co. Ltd., Japan) was attached and the finger pad. Participants experienced stimuli by touching the panel while they holded a stainless steel rod connected to the ground. The applied voltage was amplified by a voltage amplifier (HJOPS-1B20, Matsusada Precision Inc., Japan, maximum output: ± 1 kV, response: 75 kHz).

[1]The components above 3.5 Hz include frictional vibrations, such as a stick-slip vibration. Hence, the name "textural components" may be misleading. However, for convenience, we refer to the components greater than 3.5 Hz as textural components.

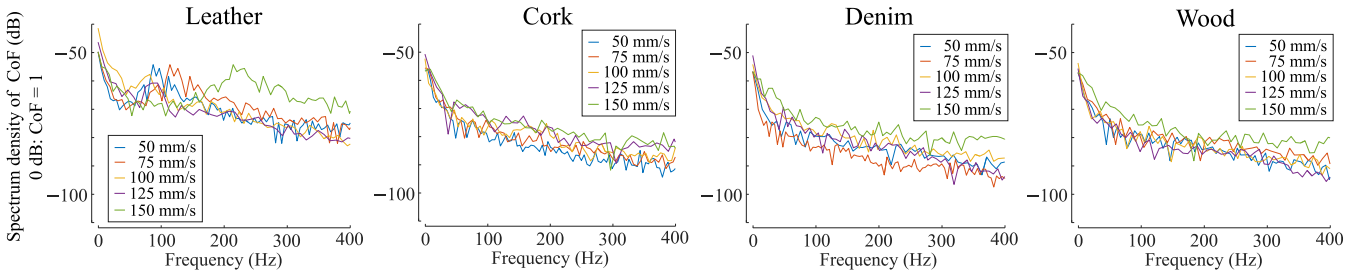

Fig. 4. Spectral density of CoF for four types of materials at five velocity levels. Estimated by autoregressive models.

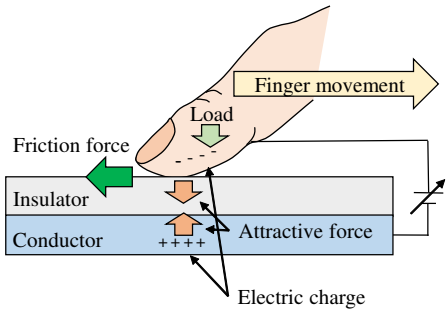

Fig. 5. Principles of electrostatic friction stimuli. The frictional force varied by controlling the electrostatic attraction force that was generated between the fingertip and the panel. The frictional force caused deformation of the fingertip in the shear direction. Adapted from [7].

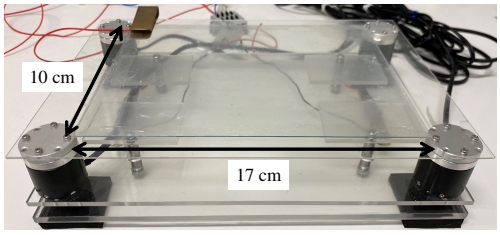

Fig. 6. Tactile texture display used in the experiments. Force sensors placed at the four corners measured the finger loads to estimate their positions.

Four force sensors (USLG25, Tec Gihan Co. Ltd., Japan) were placed under the ITO panel, and the normal force was measured in real time. The position of the finger pad was estimated from the proportion of the outputs of the four sensors. The voltage amplifier and force sensors were connected to a DAQ board (PEX-361216, Interface Corporation, Japan). The sampling frequencies were 87 Hz and 2 kHz for the force sensors and voltage outputs to the friction display, respectively.

B. Tasks

The following two tasks were conducted to compare the condition in which only the physical model for low-frequency CoF was adopted, and the condition in which the two models were adopted in conjunction. Note that the condition in which only the high-frequency textural model was adopted is not implementable because the electrostatic friction cannot lead to a negative CoF or decrease the CoF of the ITO top panel. Adjusting the base friction level [15] is not suitable for resolving this problem, because it increases the average friction level, which makes the comparison among the conditions difficult.

In Task 1, the realism of the two stimulus conditions was compared. The participants experienced the two stimulus conditions for each of the four types of materials that were presented in a randomized order. They then selected the conditions in which the virtual materials felt more realistic. Once all the materials were tested, they evaluated them again after a break of several minutes. Hence, each material was tested twice by individual participants. For the latter analysis, the mean proportions of two trials were used. During the experiment, they were able to touch natural materials and virtual stimuli as many times as they wanted, and no time limit was set.

In Task 2, the identification performance of the materials was investigated at the two stimulus conditions. The task was designed to ensure correspondence between the four types of virtual materials to the four types of actual materials for each of the two stimulus conditions. Participants could freely touch the four types of actual materials during the task. Each type of material was tested twice, and eight virtual materials were presented in a randomized order per participant at each of the two stimulus conditions. After the participants were briefed on the task, they spent a few minutes in a training session with feedback.

During Tasks 1 and 2, participants were able to move their fingers freely with no instructions on finger force and speed. Furthermore, they wore headphones and listened to pink noise.

C. Participants

Fourteen university students (males in their 20s) participated in each task after they provided written informed content. All participants were unaware of the purpose of the experiment.

D. Electrostatic friction stimuli

The relationship between the frictional force $f_s(t)$ and the applied voltage $V_e(t)$ was modeled as

$$f_s(t) = \mu\{f_n(t) + kV_e(t)^2\} \tag{5}$$

TABLE II

MEAN PROPORTIONS, 95% CONFIDENCE INTERVALS, z VALUES, AND p VALUES OF TASK 1 WHERE TWO STIMULUS CONDITIONS WERE COMPARED REGARDING THE REALISM.

	Leather	Cork	Denim	Wood
Friction + Texture	$.54 \pm .16$	$.96 \pm .07$	$.89 \pm .15$	$.54 \pm .16$
Friction only	$.46 \pm .16$	$.04 \pm .07$	$.11 \pm .15$	$.46 \pm .16$
z	.35	6.84	3.93	.35
p	1.00	4.0×10^{-16}	2.5×10^{-7}	1.00

from the law of electrostatic force and Coulomb friction[2]. μ and k are the CoF and constant related to the electrostatic force of the panel, respectively. Therefore, the applied voltage to the touch panel $V_e(t)$ was given by

$$V_e(t) = \pm\alpha\sqrt{\{\mu_p(f_n, v) + \beta\mu_t(t)\}f_n(t)}. \quad (6)$$

μ_p is the CoF of the low-frequency friction model in (3). $\mu_t(t)$ is the textural component of the CoF depending on the finger's planar velocity on the touch panel $v(t)$ and the type of material. As previously mentioned, the models of $\mu_t(t)$ were established for each of the five reference velocity levels, and the model for the reference velocity closest to the user's actual finger velocity was selected during the task. α and β represent the gains, and the authors adjusted them a priori. Furthermore, as the perception of electrostatic friction varies among individuals, the gain was adjusted for individuals near the preset values. These values were reduced when participants felt the frictions were unnaturally strong or painful, and increased when they could not perceive the frictional changes. Approximate ratios (friction component : textural component) of the applied voltages were (10:3), (10:6), (10:6), and (10:4) for leather, cork, denim, and wood, respectively. For safety reasons, stimuli above 250 V were not used. To increase the effect of electrostatic friction [17], the polarity of the applied voltages was switched at a carrier frequency of 2 kHz.

E. Results

Table II lists the results of Task 1, i.e., the mean proportions and 95% confidence intervals for the two-alternative task to select realistic stimulus condition for each of the four materials. For the leather, cork, denim, and wood, respectively, the combined low-frequency friction and high-frequency textural conditions were selected at 0.54 ± 0.16, 0.96 ± 0.07, 0.89 ± 0.15, and 0.54 ± 0.16. The table also shows the results of the z-tests to investigate whether the proportions were greater than the chance level, that is, 0.5, with p values with Bonferroni correction. For cork and denim, the combined stimulus condition was preferred. In contrast, there was no significant difference between the two stimulus conditions for the leather and wood.

Table III shows the mean proportions and 95% confidence intervals for Task 2, i.e., the material identification task, in the two stimulus conditions. In the combined condition, as shown in Table III (a), the mean correct answer proportions were 0.71 ± 0.16, 0.75 ± 0.16, 0.68 ± 0.16, and 0.82 ± 0.16 for the leather, cork, denim, and wood, respectively. Considering the confidence intervals, all materials exceeded the chance (0.25) and were correctly identified at 68–82%. As shown in Table III (b), when only the low-frequency friction stimuli were presented, the mean correct response proportions were 0.39 ± 0.18, 0.43 ± 0.19, 0.46 ± 0.21, and 0.71 ± 0.21 for the leather, cork, denim, and wood, respectively. Considering the 95% confidence interval, denim and wood were identified at proportions above the chance, but the proportions for the leather and cork were not greater than the chance level. The four types of materials were correctly identified in the range of 39–71%.

The mean correct response proportion and 95% confidence interval for all materials were 0.74 ± 0.13 for the combined condition and 0.50 ± 0.16 for the low-frequency friction condition. The identification performance was better in the case of the combined condition. Table IV summarizes the p-values when the mean correct answer proportions between the two stimulus conditions are compared with Bonferroni correction. For the leather and cork, the combined condition barely significantly improved the identification performances. Refer to Supplemental material 3 for the analyses of incorrect answer proportions.

[2]This formula may not be correct in principle; however, it formalizes the phenomenon that the frictional force is proportional to the square of the applied voltage [1], [16].

TABLE III

RESULTS OF TASK 2, IDENTIFICATION OF FOUR TYPES OF MATERIALS. MEAN ANSWER PROPORTIONS AND 95% CONFIDENCE INTERVALS FOR THE TWO STIMULUS CONDITIONS.

(a) Friction model + textural model

		Virtual materials			
		Leather	Cork	Denim	Wood
Actual materials	Leather	$.71 \pm .16$	$.00 \pm .00$	$.18 \pm .16$	$.11 \pm .11$
	Cork	$.07 \pm .09$	$.75 \pm .16$	$.11 \pm .11$	$.00 \pm .00$
	Denim	$.14 \pm .12$	$.21 \pm .13$	$.68 \pm .16$	$.07 \pm .09$
	Wood	$.07 \pm .09$	$.04 \pm .07$	$.04 \pm .07$	$.82 \pm .16$

(b) Friction model

		Virtual materials			
		Leather	Cork	Denim	Wood
Actual materials	Leather	$.39 \pm .18$	$.14 \pm .12$	$.36 \pm .18$	$.11 \pm .11$
	Cork	$.46 \pm .23$	$.43 \pm .19$	$.04 \pm .07$	$.04 \pm .07$
	Denim	$.11 \pm .11$	$.36 \pm .18$	$.46 \pm .21$	$.14 \pm .05$
	Wood	$.04 \pm .07$	$.07 \pm .09$	$.14 \pm .15$	$.71 \pm .21$

TABLE IV

MEAN PROPORTIONS, 95% CONFIDENCE INTERVAL, z VALUES, AND p VALUES OF TASK 2 WHERE TWO STIMULUS CONDITIONS WERE COMPARED REGARDING THE IDENTIFICATION.

	Leather	Cork	Denim	Wood
Friction + Texture	$.71 \pm .16$	$.75 \pm .16$	$.68 \pm .16$	$.82 \pm .16$
Friction only	$.39 \pm .18$	$.43 \pm .19$	$.46 \pm .21$	$.71 \pm .21$
z	2.58	2.58	1.95	1.29
p	.04	.04	.20	.77

V. Discussion

The present study found that the effects of the combined model depended on the type of materials whereas our previous study [7] showed that the virtual materials could be more discriminable from each other by using the combined model. The materials can be divided in three groups based on the results of Tasks 1 and 2. The first group comprises the cork and denim. By using the combined model, both the realism and identification accuracies were improved, although the improvement for the identification accuracy for denim was not statistically significant. For these materials with rough surfaces, the textural model is thought to be necessary, and the combined stimuli were effective. The second group comprised the leather. By using the combined stimuli, the realism of the leather did not change, whereas the leather exhibited the highest friction forces and was easily separated from other materials. According to the introspective reports from the participants, the virtual leather was not realistic because of the lack of the typical softness of leather. The third group comprised wood for which the combined stimuli did not improve the realism and identification performance. Its surface was largely smooth, and its tactile feelings were mostly determined by its frictional properties. Hence, the presence or absence of the textural model did not make a significant difference to the performance of the two tasks. In Task 2, participants could identify the wood with high probability even at friction-only model potentially because its exponential power b was the lowest among the four types of materials and the friction force rarely depended on the normal force.

There exist some issues and limitations which need to be solved in the future. Our friction model in Section III-A does not capture the changes in the measured low-frequency CoF with high precision partly because the effects of dynamic finger motions, such as acceleration, were not considered. The friction model may need to embrace the effects of static friction, whereas only the kinetic friction was modeled in this study. In addition, we determined the order of AR models on the basis of Akaike Information Criteria. This approach might not have accurately produced low-frequency components. The method to determine the order for tactile texture rendering remains to be studied. Although it is unclear which of these factors is the most important for texture perception, it may improve the quality of surface texture displays. Furthermore, it is interesting to compare the results of the present study and our past study [7] underlining the present rendering methods. However, the direct comparison is difficult because of the inherent differences in the user experiments in the two studies.

VI. Conclusion

We developed a texture rendering method for electrostatic friction surface displays. The method combined a physical model for low-frequency frictional components (0–3.5 Hz) and a data-driven textural model for high-frequency frictional components (> 3.5 Hz). Many earlier data-driven methods did not aim at covering such a wide frequency range for these types of texture displays. We tested the efficacy of the combined rendering method by comparing it with a method that adopted only low-frequency frictional components. Two user studies revealed that the developed method increased the perceived realism and identification rates for material textures, and was especially effective for non-soft textured surfaces, such as cork and denim. This method is expected to improve the quality of material textures for use in electrostatic surface displays.

References

[1] C. Basdogan, F. Giraud, V. Levesque, and S. Choi, "A review of surface haptics: Enabling tactile effects on touch surfaces," *IEEE Transactions on Haptics*, vol. 13, no. 3, pp. 450–470, 2020.

[2] G. Ilkhani, M. Aziziaghdam, and E. Samur, "Data-driven texture rendering on an electrostatic tactile display," *International Journal of Human-Computer Interaction*, vol. 33, no. 9, pp. 756–770, 2017.

[3] R. Haghighi Osgouei, J. R. Kim, and S. Choi, "Data-driven texture modeling and rendering on electrovibration display," *IEEE Transactions on Haptics*, vol. 13, no. 2, pp. 298–311, 2020.

[4] H. Culbertson, J. Unwin, and K. J. Kuchenbecker, "Modeling and rendering realistic textures from unconstrained tool-surface interactions," *IEEE Transactions on Haptics*, vol. 7, no. 3, pp. 381–393, 2014.

[5] R. Hassen and E. Steinbach, "Vibrotactile signal compression based on sparse linear prediction and human tactile sensitivity function," in *Proceedings of IEEE World Haptics Conference*, 2019, pp. 301–306.

[6] H. Culbertson and K. J. Kuchenbecker, "Importance of matching physical friction, hardness, and texture in creating realistic haptic virtual surfaces," *IEEE Transactions on Haptics*, vol. 10, no. 1, pp. 63–74, 2017.

[7] K. Otake, S. Okamoto, Y. Akiyama, and Y. Yamada, "Virtual tactile texture using electrostatic friction display for natural materials: The role of low and high frequency textural stimuli," in *Proceedings of IEEE International Conference on Robot and Human Interactive Communication*, 2021, pp. 392–397.

[8] H. Hasegawa, S. Okamoto, and Y. Yamada, "Phase difference between normal and shear forces during tactile exploration represents textural features," *IEEE Transactions on Haptics*, vol. 13, no. 1, pp. 11–17, 2020.

[9] H.-J. Freund, "Time control of hand movements," in *The Oculomotor and Skeletalmotor Systems: Differences and Similarities*, ser. Progress in Brain Research, 1986, vol. 64, pp. 287–294.

[10] K. Inoue, S. Okamoto, Y. Akiyama, and Y. Yamada, "Effect of material hardness on friction between a bare finger and dry and lubricated artificial skin," *IEEE Transactions on Haptics*, vol. 13, no. 1, pp. 123–129, 2020.

[11] S. Derler, L.-C. Gerhardt, A. Lenz, E. Bertaux, and M. Hadad, "Friction of human skin against smooth and rough glass as a function of the contact pressure," *Tribology International*, vol. 42, no. 11, pp. 1565–1574, 2009.

[12] M. J. Adams, S. A. Johnson, P. Lefevre, V. Levesque, V. Hayward, T. Andre, and J.-L. Thonnard, "Finger pad friction and its role in grip and touch," *Journal of The Royal Society Interface*, vol. 10, no. 80, p. 20120467, 2013.

[13] R. Hassen and E. Steinbach, "Subjective evaluation of the spectral temporal similarity (ST-SIM) measure for vibrotactile quality assessment," *IEEE Transactions on Haptics*, vol. 13, no. 1, pp. 25–31, 2020.

[14] C. M. Greenspon, K. R. McLellan, J. D. Lieber, and S. J. Bensmaia, "Effect of scanning speed on texture-elicited vibrations," *Journal of The Royal Society Interface*, vol. 17, no. 167, p. 20190892, 2020.

[15] R. Haghighi Osgouei, J. R. Kim, and S. Choi, "Improving 3D shape recognition with electrostatic friction display," *IEEE Transactions on Haptics*, vol. 10, no. 4, pp. 533–544, 2017.

[16] E. Vezzoli, W. B. Messaoud, M. Amberg, F. Giraud, B. Lemaire-Semail, and M. Bueno, "Physical and perceptual independence of ultrasonic vibration and electrovibration for friction modulation," *IEEE Transactions on Haptics*, vol. 8, no. 2, pp. 235–239, 2015.

[17] T. Nakamura and A. Yamamoto, "Modeling and control of electroadhesion force in dc voltage," *Robomech Journal*, vol. 4, no. 1, p. 18, 2017.